

Molecular Physics

An International Journal at the Interface Between Chemistry and Physics

ISSN: 0026-8976 (Print) 1362-3028 (Online) Journal homepage: <http://www.tandfonline.com/loi/tmph20>


Theoretical analysis of the experimental UV-Vis absorption spectra of some phenolic Schiff bases

Jelena Đorović, Zoran Marković, Zorica D. Petrović, Dušica Simijonović & Vladimir P. Petrović

To cite this article: Jelena Đorović, Zoran Marković, Zorica D. Petrović, Dušica Simijonović & Vladimir P. Petrović (2017) Theoretical analysis of the experimental UV-Vis absorption spectra of some phenolic Schiff bases, *Molecular Physics*, 115:19, 2460-2468, DOI: [10.1080/00268976.2017.1324183](https://doi.org/10.1080/00268976.2017.1324183)

To link to this article: <http://dx.doi.org/10.1080/00268976.2017.1324183>

 View supplementary material [↗](#)

 Published online: 10 May 2017.

 Submit your article to this journal [↗](#)

 Article views: 39

 View related articles [↗](#)

 View Crossmark data [↗](#)

Full Terms & Conditions of access and use can be found at
<http://www.tandfonline.com/action/journalInformation?journalCode=tmph20>

RESEARCH ARTICLE



Theoretical analysis of the experimental UV-Vis absorption spectra of some phenolic Schiff bases

Jelena Đorović^a, Zoran Marković^{a,b}, Zorica D. Petrović^c, Dušica Simijonović^c and Vladimir P. Petrović^c

^aBioengineering Research and Development Center, Kragujevac, Republic of Serbia; ^bDepartment of Chemical-Technological Sciences, State University of Novi Pazar, Novi Pazar, Republic of Serbia; ^cDepartment of Chemistry, Faculty of Science, University of Kragujevac, Kragujevac, Serbia

ABSTRACT

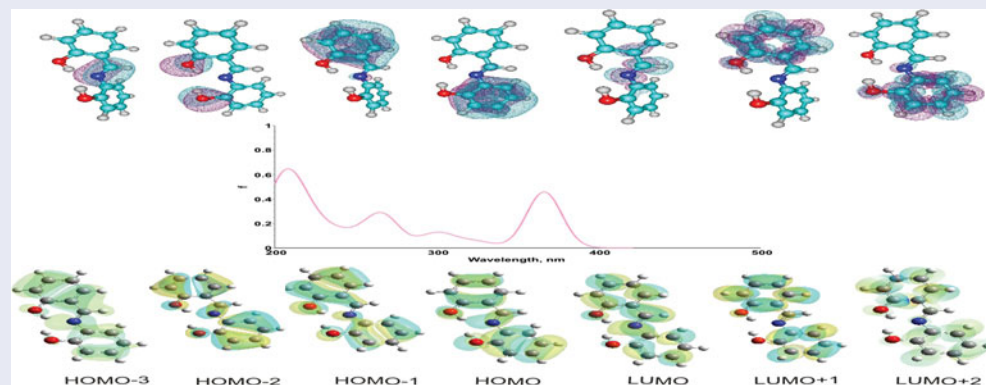
The time-dependent density functional theory (TDDFT) was applied in conjunction with the natural bond orbital analysis to examine the UV-Vis properties of 10 phenolic Schiff bases. The calculations were performed with different functionals, but main discussion refers to results obtained at the B3LYP/6-311+G(d,p) level of theory. The approach based on the natural localised molecular orbital clusters indicates similar behaviour for majority of examined compounds. The HOMO (“highest occupied molecular orbital”) cluster is delocalised over the ring which is electron richer, the HOMO-1 cluster is spread over the other ring, whereas the LUMO (“lowest unoccupied molecular orbital”) cluster is situated on the imino group. The two bands at long wavelengths correspond to the HOMO → LUMO and HOMO-1 → LUMO transitions, i.e. from both A and B rings to the imino group. The next band originates from a transition from the imino group to the imino group. The band at the smallest wavelengths originates from a transition from the A ring to the A ring, or from the B ring to the B ring. Our findings are in very good agreement with the existing literature data.

ARTICLE HISTORY

Received 24 February 2017
Accepted 21 April 2017

KEYWORDS

Schiff bases; UV-Vis spectra; TDDFT; NLMO clusters





Introduction

Free radicals and other reactive species are constantly generated in the human body. Although oxygen is crucial for aerobic organisms, it also represents one of the main inter-gradients for production of reactive oxygen species (ROS) [1]. An imbalance between the production of ROS and a biological system's ability to readily detoxify reactive intermediates, or repair the resulting damage causes oxidative stress. It is considered that oxidative stress plays an important role in the pathogenesis of many diseases including inflammation,

cancer, hypertension, diabetes mellitus, atherosclerosis, ischemia/reperfusion injury, neurodegenerative disorders, rheumatoid arthritis and ageing [2–6].

The organisms have developed a variety of the internal defence mechanisms to neutralise damaging effect of free radicals which are grouped as enzymatic and non-enzymatic systems [1]. There are also some external factors which can act as scavengers. Numerous examples of successful use of antioxidants to reduce the pathological consequences of oxidative stress have been reported, and they include dietary substances, such as flavonoids,

CONTACT Jelena Đorović  jelena.djorovic@kg.ac.rs

 Supplemental data for this article can be accessed at  <http://dx.doi.org/10.1080/00268976.2017.1324183>.

© 2017 Informa UK Limited, trading as Taylor & Francis Group

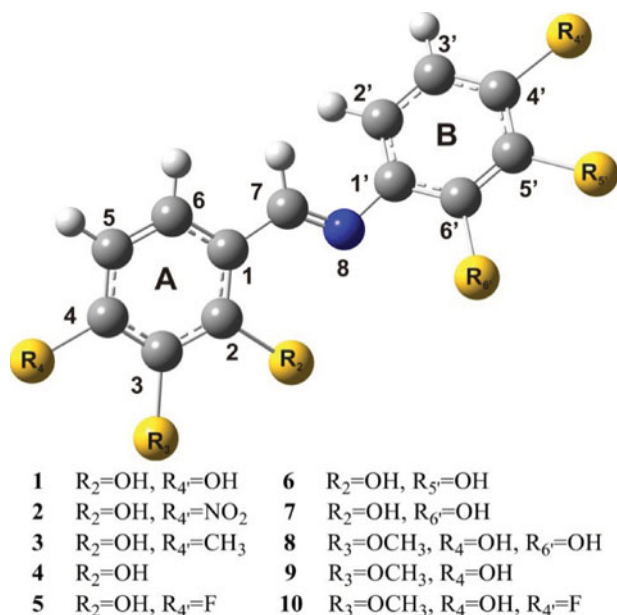


Figure 1. General structure of the compounds under investigation.

phenolic acids, vitamins C and E, hydroquinones and various sulphhydryl compounds which help in preventing free radical damage. A possible association between the consumption of foods containing phenolic compounds, and a reduced risk of developing disorders, such as cancer and cardiovascular diseases, has been evaluated in several epidemiological investigations [7–10]. Both, natural and synthetic (poly)phenolic compounds have been characterised for their antioxidant activity [11–13]. Schiff bases containing hydroxy group as a substituent on the phenyl ring are part of the group of synthetic phenolic compounds [14]. This group of chemicals found wide range of applications in medicine and pharmacy through their antitumour, antiviral, antifungal and antibacterial activities [15–17]. Also, it has been reported that salicylaldehyde Schiff bases act as antimicrobial agents [18–20]. Furthermore, some phenolic Schiff bases show effective antioxidant activity, and therefore are potent as medicals which can prevent diseases caused by free radical damage [21,22]. Recently, we reported the antioxidative properties of some salicylaldehyde and vanillic-based Schiff bases [23,24]. In the further course of our work, we devoted our efforts towards determination of the UV-Vis properties of the series of synthetic Schiff bases (Figure 1).

UV-Vis absorption properties of π conjugated phenolic compounds depend on the chemical structure, especially on the number and position of the π electron pair donating groups, such as hydroxy, methoxy and glycoside [25]. The quantum-chemical interpretation of the UV-Vis spectra of the compounds containing these functional groups is of crucial importance in supplementing experimental data. Namely, quantum chemistry

opens possibility to understand the direct correlation of optical properties with the fundamental chemical structure through the molecular orbital description. Among the quantum chemical methods used for explanation of UV-Vis absorbing properties, the time-dependent density functional theory (TDDFT) arises as an effective tool, especially for estimation of UV-Vis absorption of medium-sized π conjugated compounds [26].

In a recent paper, Marković *et al.* combined the TDDFT and natural bond orbital (NBO) theories to provide better understanding of the UV-Vis absorption of anthraquinones, neoflavonoids and flavonoids, by constructing their NLMO (natural localised molecular orbital) clusters [27]. Following similar methodology, we investigated the UV-Vis spectra of the Schiff bases 1–10 (Figure 1). Our study confirmed the findings of Marković *et al.* that the results from the TDDFT and NBO theories can be complementarily used to interpret and understand the UV-Vis spectra.

Methodology section

Experimental

The UV-Vis measurements were performed at room temperature in the area of 200–500 nm range on the Agilent Technologies, Cary 300 series UV-Vis spectrophotometer. The solutions (2.5×10^{-5} M concentration) of all compounds (1–10) were prepared in methanol, and measurements were recorded in a 10 mm quartz cell.

Computational methods

All calculations were carried out using the Gaussian program package [28] with B3LYP, M05-2X and PBE0 methods in conjugation with 6-311+G(d,p) basis set [29–32]. The geometries of all 10 Schiff bases in methanol were fully optimised, and frequency calculations performed, to ascertain the nature of the critical point as true minimum. The absorption spectra were computed using the TDDFT method in combination with the same functional, basis set and solvation model. For simulation of effects of methanol solvent, two approaches have been utilised: implicit solvation model simulated by the Conductor-like Polarizable Continuum Model (dielectric constant = 32.6) [33], and explicit methanol molecules. The number of included methanol molecules depends on possible hydrogen bonding sites available in each molecule.

All allowed vertical transitions ($\pi \rightarrow \pi^*$ and $n \rightarrow \pi^*$) were inspected, and the resultant wavelengths (max) and oscillator strengths (f) were determined. The NBO analysis was performed for all examined compounds.

Following the procedure described in [27], the NLMO clusters were constructed for Schiff bases.

Results and discussion

There are few papers devoted to the UV-Vis absorption of Schiff bases [34–36]. It has been commonly accepted that the bands in the range of 300–350 nm involve $\pi \rightarrow \pi^*$ transitions of the C = N group, whereas the bands in the range of 210–400 nm may be attributed to $\pi \rightarrow \pi^*$ and $n \rightarrow \pi^*$ transitions of the aromatic rings [34,35]. However, the question ‘what gets excited to where’ still requires an answer. In a paper of Amati *et al.*, devoted to the determination of the configuration of C = N bond in some heteroaryl imines, UV-Vis spectroscopy was one of the used techniques. It was found that the intense band at long wavelengths can be considered as a HOMO \rightarrow LUMO transition where ‘the excited state should involve both the iminic bridge and the aromatic rings’ [37].

To provide deeper insight into UV-Vis absorption of this class of compounds, we performed an investigation based on both TDDFT method and NLMO clusters analysis. The optimised geometries of the 10 examined compounds are depicted in Figure S1. In all cases, the B ring slightly deviates from the plane formed by the A ring and imino group. An analysis of the parent NBOs of all compounds revealed that the lone pair on N8 is sp^2 hybridised. There are significantly small occupancies in the π orbitals and lone pairs on the oxygen and nitrogen atoms, and notably large occupancies in some antibonding NBOs (see Tables S1 and S2). This condition is a consequence of donation of electron density from these π , p and sp^2 NBOs into the adjacent π^* antibonding orbitals, and is in accordance with a familiar chemical picture of conjugated systems. An interesting donor–acceptor interaction is involved in O–H...N hydrogen bond, which is formed between the nitrogen of the imino group and hydrogen of the hydroxyl group attached to aromatic ring (A, B or both). Here, electron density is donated from the sp^2 orbital of N8 into the proximate σ^* antibonding H–O orbital. To establish hydrogen bonds between hydroxyl group and electron pair from π orbital of imino group, Schiff bases 1–6 form 6-membered ring, 8 forms 5-membered, 7 forms both of them, while 9 and 10 lack such intramolecular interactions. As expected, the 6-membered hydrogen bonds are much stronger than the 5-membered ones, which are manifested through their lengths of around 1.7 and 2.0 Å, respectively. Compound 4 has no other substituents; 2 has an electron withdrawing nitro group and 3 has an electron donating methyl group. The substituents on all other molecules exhibit negative inductive, but positive resonance effects. Certainly, all compounds contain an iminic bridge. On the

Table 1. Experimental and TDDFT results for examined compounds. λ_{\max} denotes experimental and calculated wavelengths, and f stands for oscillator strength.

Comp.	λ_{\max} (nm)		f	Orbital description
	Exp	Calc		
1	349	357	0.68	H \rightarrow L (70%)
	321 (sh) ^a	315	0.04	H-1 \rightarrow L (68%)
	269	272	0.15	H-3 \rightarrow L (46%)
	231	241	0.12	H \rightarrow L+2 (50%)
2	353	356	0.51	H-1 \rightarrow L (70%)
	318	319	0.04	H \rightarrow L+1 (48%)
	212	230	0.08	H \rightarrow L+3 (53%)
3	339	347	0.63	H \rightarrow L (69%)
	317 (sh) ^a	313	0.08	H-1 \rightarrow L (68%)
	269	271	0.22	H-3 \rightarrow L (56%)
	225	236	0.13	H \rightarrow L+2 (50%)
4	337	340	0.50	H \rightarrow L (69%)
	315 (sh) ^a	310	0.14	H-1 \rightarrow L (67%)
	268	270	0.25	H-3 \rightarrow L (59%)
	221	223	0.12	H \rightarrow L+2 (58%)
5	337	342	0.51	H \rightarrow L (69%)
	314 (sh) ^a	310	0.14	H-1 \rightarrow L (67%)
	269	269	0.11	H-3 \rightarrow L (44%)
	221	232	0.10	H-1 \rightarrow L+1 (52%)
6	340	345	0.48	H \rightarrow L (70%)
	266	270	0.30	H-3 \rightarrow L (58%)
	229 (sh) ^a	240	0.09	H \rightarrow L+2 (51%)
7	349	366	0.46	H \rightarrow L (70%)
	268	266	0.28	H-3 \rightarrow L (58%)
8	234 (sh) ^a	243	0.05	H \rightarrow L+2 (58%)
	350	371	0.75	H \rightarrow L (69%)
	315 (sh) ^a	318	0.11	H-1 \rightarrow L (68%)
9	283	285	0.07	H-3 \rightarrow L (56%)
	232	248	0.11	H \rightarrow L+2 (63%)
	325	339	0.73	H \rightarrow L (66%)
	284	279	0.12	H-2 \rightarrow L (59%)
10	227	239	0.10	H \rightarrow L+2 (39%)
	327	340	0.74	H \rightarrow L (67%)
	284	279	0.12	H-2 \rightarrow L (58%)
	232	234	0.06	H-1 \rightarrow L+1 (59%)

^ash: shoulder.

basis of the partial positive charge on C7 and partial negative charge on N8, one can conclude that the imino group withdraws electron density from the A ring and donates it to the B ring.

The UV-Vis spectra of these 10 Schiff bases were recorded, and simulated by means of the TDDFT calculations. The obtained experimental and theoretical data: vertical transition wavelength (λ_{\max}), oscillator strength (f) and orbital contribution coefficient values for all absorption bands are listed in Table 1. UV-Vis spectra were simulated using three different functionals (B3LYP, M05-2X and PBE0) [38]. M05-2X method either failed to reproduce UV-Vis spectra bands, or they were significantly shifted (Figure S2). It was expected since M06-2X functional also not reproduce well experimental UV-Vis spectra and underestimates the λ_{\max} values [27]. Other functionals repeated experimental bands with sufficient accuracy. To decide which data will be presented here, average absolute and relative errors, as well as for the correlation coefficients were determined (Figure S3). For

the cases where two or more calculated electronic transitions were affiliated with a single experimental band, the mean value is calculated and assigned to the experimental one. The experimental and calculated wavelengths form straight lines with the correlation coefficients of 0.982 (B3LYP) and 0.978 (PBE0, Figure S3). Discrepancy between the experimental and calculated results is notable at short wavelengths. Based on the correlation coefficients and absolute and relative error values, both functionals in combination with TDDFT method reproduced quite well the UV-Vis spectra of investigated compounds. However, it is prominent that results obtained with B3LYP functional are slightly in better agreement, and because of that, all further discussion will be referred to the B3LYP results. In addition to this, some other authors concluded that B3LYP achieved the best agreement with experimental results [27,38].

In Figure 2, the experimental and simulated spectra for the two representatives of the investigated Schiff bases, compounds 2 and 3, are illustrated, while all other spectra

are provided in Figure S4. These molecules were selected because the only structural difference between them is that the substituent in the para position of the B ring is electron withdrawing in 2, and electron donating in 3.

Figures 2 and S4 show that both experimental and simulated spectra for all investigated compounds are mutually very similar. In general, the investigated Schiff bases have three intensive bands in the regions of 335–350, 265–285 and 220–235 nm, and a shoulder in the range of 310–325 nm. The similarity among the UV-Vis spectra of all examined Schiff bases is not surprising, since structural differences among them are not pronounced. Thus, an explanation of subtle dissimilarity caused by fine structural differences is a challenging task. To gain deeper insight into the UV-Vis properties of the examined compounds, the Kohn–Sham orbitals and corresponding NLMO clusters were constructed for the compounds 1–10. All data necessary for the construction of the NLMO clusters for the compounds 2 and 3 are presented in Tables S1 and S2, and the results are depicted in

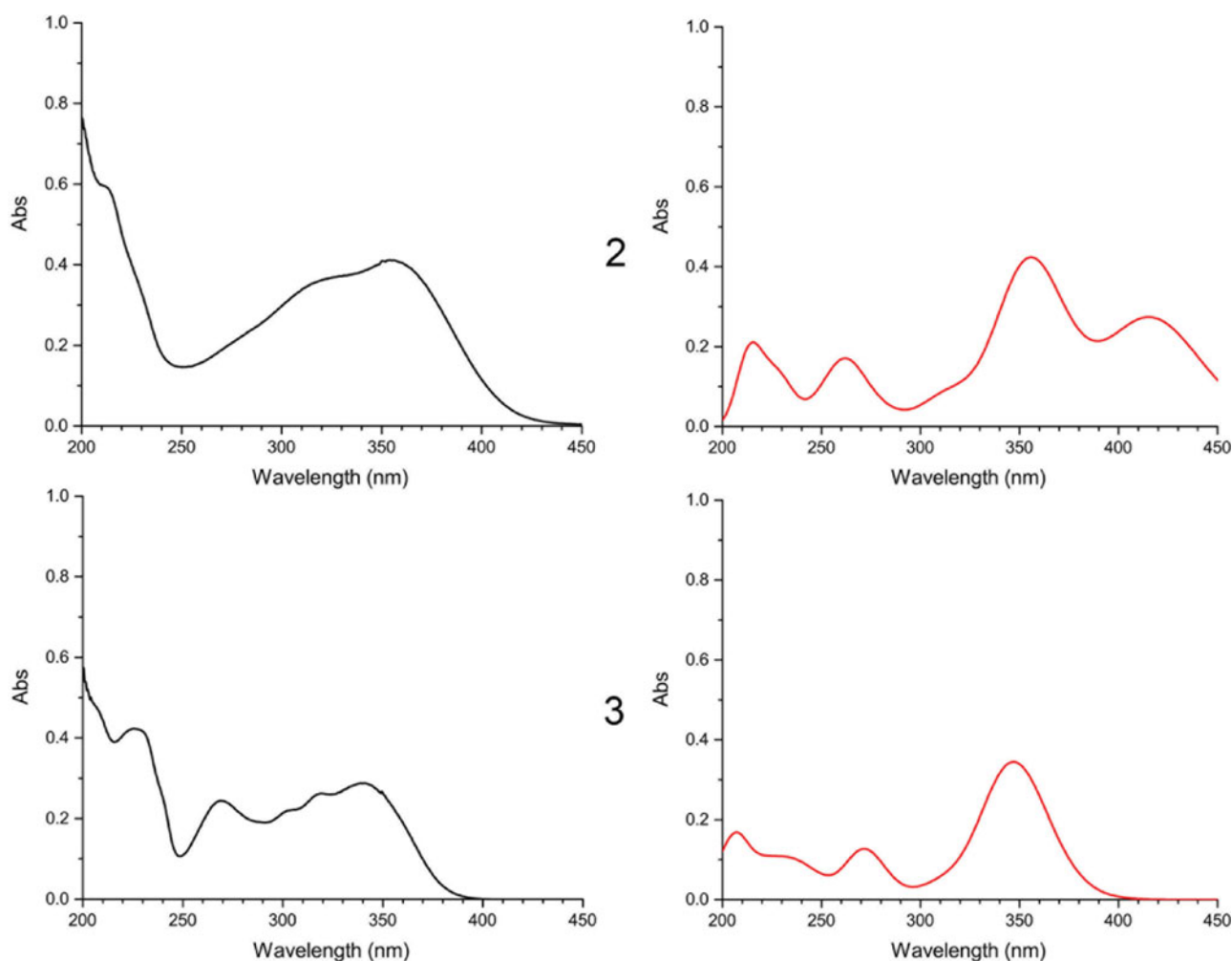


Figure 2. Experimental (left) and simulated (right) UV-Vis spectra for compounds 2 and 3.

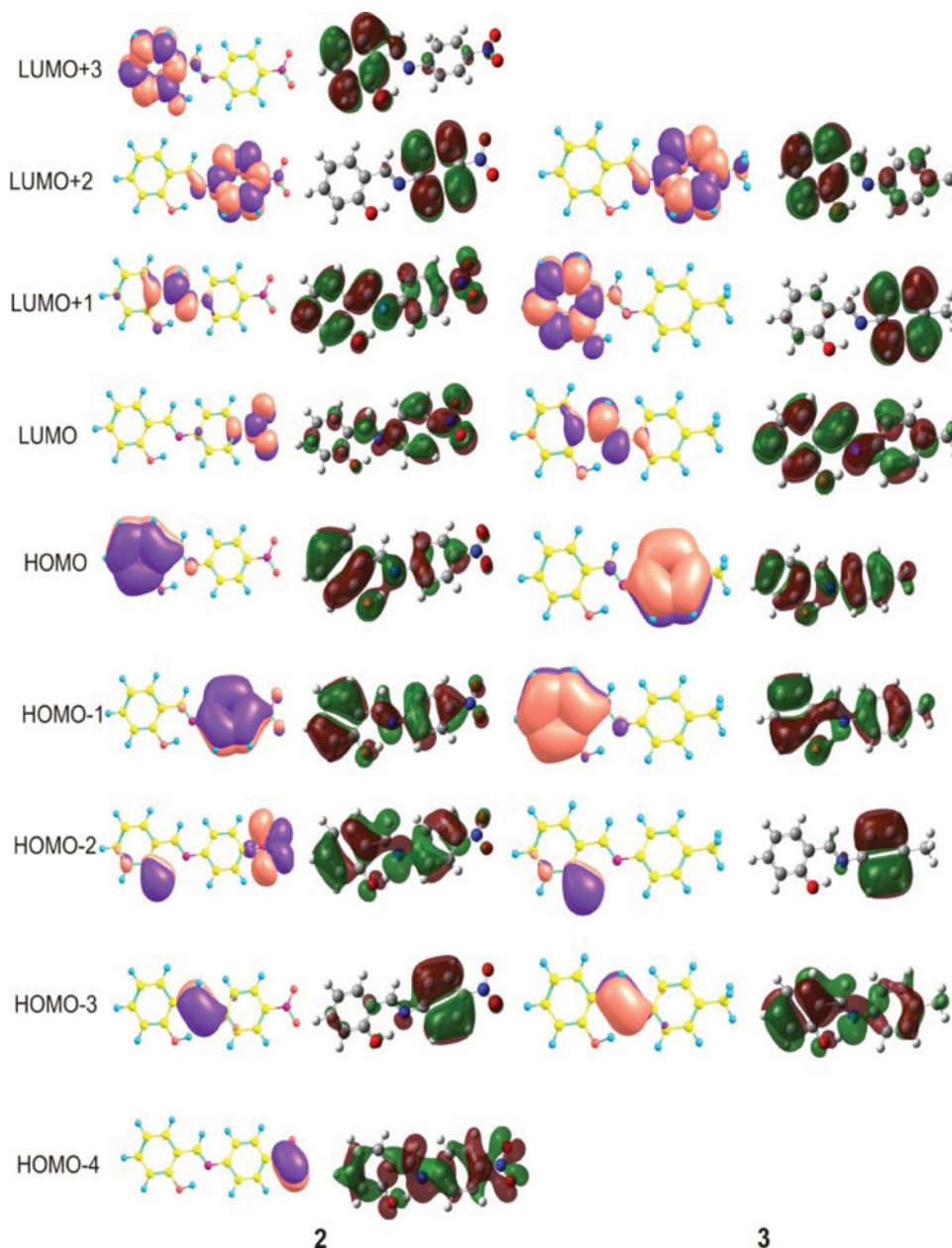


Figure 3. NLMO clusters (left) and corresponding Kohn–Sham orbitals (right) for the compounds 2 and 3.

Figure 3. The corresponding results for 5 and 8 are given in Figures S5 and S6.

It is clear from Table S2 that in the bonding region of 3, the π NLMO from the C = N group has the lowest energy value. This NLMO forms the lowest-lying HOMO-3 cluster (**Figure 3**). The HOMO-2 cluster is composed of the lone electron pair in the p orbital of the hydroxyl oxygen. Three π NLMOs from the A ring are of the same nature, and are characterised with small spatial and energetic separations, implying that they compose the HOMO-1 cluster. Similarly, the HOMO cluster consists of three π NLMOs from the B ring. In the antibonding region, the LUMO cluster is formed from the π^* orbital of the

C = N group. The LUMO+1 cluster is built from three π^* NLMOs of the A ring, while three π^* NLMOs of the B ring create the LUMO+2 cluster. It turns out that the HOMO cluster of 3 is spread over the B ring, whereas the HOMO-1 cluster is delocalised over the A ring. This occurrence is, certainly, a consequence of the fact that electron releasing methyl group increases electron density in the B ring, and facilitates electron excitation.

Table S1 and **Figure 3** show that the lowest-energy NLMO clusters in both bonding and antibonding regions of 2 are spread over the nitro group (HOMO-4 and LUMO clusters). The HOMO-3, HOMO-2, HOMO-1 and HOMO clusters of 2 are of similar compositions as

the corresponding NLMO clusters of 3. In addition, the LUMO+1, LUMO+2 and LUMO+3 clusters of 2 are analogous to the LUMO, LUMO+1 and LUMO+2 clusters of 3. A significant difference between the NLMO clusters of 2 and 3 is that in 2 the HOMO and LUMO+3 clusters are delocalised over the A ring, whereas the HOMO-1 and LUMO+2 clusters are delocalised over the B ring. The origin of this difference is the nature of the substituent on the B ring. Electron withdrawing nitro group decreases electron density in the B ring, thus making the A ring more favourable molecular moiety for electron excitation at long wavelengths.

The Kohn–Sham orbitals are in majority of cases delocalised over the entire molecular skeletons, and their shapes are not helpful in answering some crucial questions on molecular moieties involved in electronic transitions, possible intramolecular charge transfer, etc. Taking into account the fact that the NLMO clusters are delocalised over the definite parts of molecules, we will now try to provide necessary answers by substituting the Kohn–Sham orbitals with the corresponding NLMO clusters [27]. We will first discuss the UV-Vis spectrum of compound 3 on the basis of the results presented in Table 1 and Figure 3. According to the TDDFT theory, the experimental band at 339 nm is predicted at 347 nm, and it engages a HOMO \rightarrow LUMO transition. An analysis based on the NLMO clusters describes this transition as a $\pi \rightarrow \pi^*$ transition from the B ring to the imino group (HOMO \rightarrow LUMO). This transition involves a favourable intramolecular charge transfer, and the large f value for this band is a consequence of the small spatial and energetic separations. The next band at 317 nm corresponds to a $\pi \rightarrow \pi^*$ transition from the A ring to the imino group (HOMO-1 \rightarrow LUMO). This transition also involves an intramolecular charge transfer over the conjugated molecular moiety, but owing to the larger energetic separation the f value for this transition is small, and agrees with the experimental fact that this transition appears as a shoulder. The next band at 269 nm corresponds to a $\pi \rightarrow \pi^*$ transition from the imino group to the imino group (HOMO-3 \rightarrow LUMO). Finally, the band at 225 nm can be ascribed to a $\pi \rightarrow \pi^*$ transition from the B ring to the B ring (HOMO \rightarrow LUMO+2). In spite of the large energetic separations, these two electronic transitions are spatially very favourable, and are characterised with relatively large f values. In the case of the Schiff base 2, the TDDFT calculation predicted an intensive band at 417 nm which corresponds to a HOMO \rightarrow LUMO transition, but does not have a match in the experimental spectrum (Figure 2). Instead, a HOMO-1 \rightarrow LUMO transition is predicted at 356 nm to simulate the experimental band at 353 nm. If Table 1 is carefully inspected, it will become clear that only the

compound 2 shows completely different pattern from all other Schiff bases. Figure 3 shows that the LUMO cluster is positioned on the nitro group of 2, whereas the HOMO and HOMO-1 clusters are delocalised over the A and B rings, respectively. Due to particularly large spatial separation between the HOMO and LUMO clusters, a $\pi \rightarrow \pi^*$ transition from the B ring to the nitro group of 2 (HOMO-1 \rightarrow LUMO) turns out to be more favourable electron transition in spite of the larger energetic separation. The next band at 318 nm can be attributed to a $\pi \rightarrow \pi^*$ transition from the A ring to the imino group (HOMO \rightarrow LUMO+1); and finally, the band at 212 nm can be ascribed to a $\pi \rightarrow \pi^*$ electronic transition from the A ring to the A ring. Both transitions involve larger energetic separations, and the former involves small spatial separation. Therefore, these two transitions are characterised with relatively small oscillator strength values.

It is important to emphasise that in the case of vanillin originating Schiff bases 9 and 10, bands around 280 nm are not consequence of HOMO-3 \rightarrow LUMO transition as in the case of structurally similar compound 8. Here, HOMO-2 \rightarrow LUMO electron transition is responsible for the appearance of these bands. All bands in compounds 8, 9 and 10 are consequences of $\pi \rightarrow \pi^*$ electronic transition, except the bands around 280 nm in 9 and 10 which can be ascribed to the $n \rightarrow \pi^*$ transition. This behaviour can be attributed to the different substitution in the ring B of these molecules. Namely, although in all three cases there are hydroxy and methoxy groups in the ring A, the effects of the *ortho*-hydroxy group in the ring B seem to be prevailing factor for the electron transition for this band.

To make a broader picture of the UV-Vis absorption of the examined Schiff bases, the NLMO clusters for all compounds were examined carefully. At first glance, one can see that spectra of all Schiff bases (except compound 2) show very similar patterns. The HOMO cluster is spread over the A or B ring, which depends on which of them is electron richer. Then, the HOMO-1 cluster is delocalised over the ring of smaller electron density. Taking into account that both rings have substituents with different inductive and resonance effects, their influence to the electron density of the rings is unpredictable. This problem will be illustrated with the partial charges in the simplest Schiff base 4, which lacks any groups on the B ring (Figure 4).

The *ortho* and *para* carbons of the B ring are characterised with slightly larger negative NBO charges in comparison to the *meta* positions, which confirms weak positive resonance effect of the imino group. On the other hand, a positive partial charge on C1' demonstrates negative inductive effect of the nitrogen. Increased partial negative charges on C3 and C5 (*ortho* and *para*) are the consequence of the positive resonance effect of

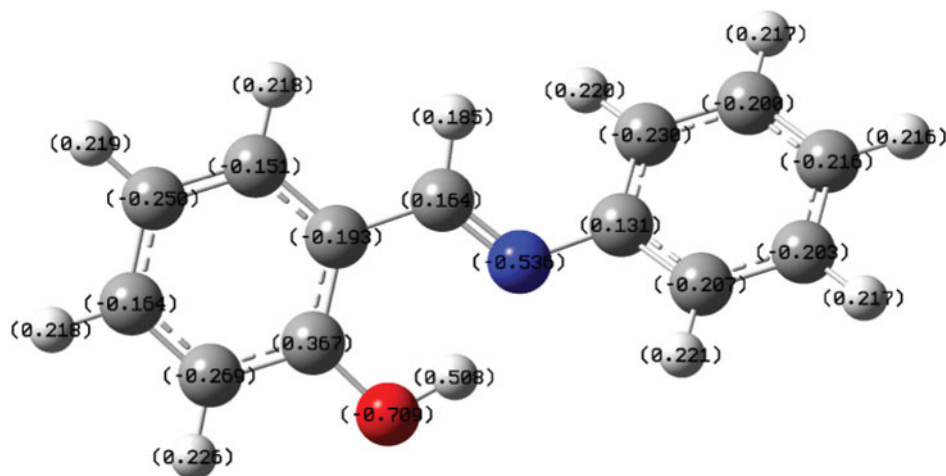


Figure 4. Distribution of the NBO charges in the Schiff base 4.

the hydroxyl group. The negative NBO charge on C1 (another ortho) is notably smaller because it suffers electron withdrawing effect of the imino group. C2 bears a large partial positive charge which can be attributed to the negative inductive effect of the oxygen. Taking into account that the situation in other molecules is even more complex, we supposed that electron density in a ring can be estimated on the basis of the sum of the partial charges on the constituting carbon atoms. These sums were calculated for the compounds 1–10, and their values are presented in Figure S1. Our assumption is that the larger negative sum of the NBO charges indicates that the corresponding ring is characterised with larger electron density, which further implies that the HOMO cluster will be delocalised over this ring. Then, the HOMO-1 cluster will be spread over the other ring. An inspection of these values shows that the sum of the NBO charges on the carbons takes larger negative value in the B ring only in the cases of 3, 4, 8, 9 and 10. In all other molecules, the A ring is characterised with larger negative sum of the partial charges on the carbon atoms. This finding is in perfect agreement with the analysis based on the NLMO clusters. Namely, in the Schiff bases 3, 4 and 8, the HOMO cluster is spread over the B ring, and HOMO-1 cluster is spread over the A ring (3 in Figure 3 and 8 in Figure S6 illustrate such behaviour). In the compounds 1, 2 and 5–7, the HOMO cluster is delocalised over the A ring, whereas the HOMO-1 cluster is delocalised over the B ring (2 in Figure 3 and 5 in Figure S5 are given as examples).

A common feature of all examined molecules is that the LUMO cluster is composed of the π^* orbital of the imino group. The only exception is the base 2 whose LUMO is positioned on the nitro group. Since different behaviour of 2 has already been explained, it will be excluded from the current discussion. If one recalls

Table 1, they will conclude that the two bands at long wavelengths correspond to the HOMO \rightarrow LUMO and HOMO-1 \rightarrow LUMO transitions, i.e. from both rings to the imino group. Our results regarding these two bands are in excellent agreement with the finding of Amati *et al.* [37] who concluded that both the iminic bridge and aromatic rings are involved in a transition at long wavelengths. The next band originates from a transition from the imino group to the imino group. Finally, the band at the largest excitation energy results from a transition from the A ring to the A ring (molecules 1, 2, 6 and 7) or from the B ring to the B ring (molecules 3, 4, 5 and 8).

In addition to simulated spectra with implicit solvent, we performed simulation with explicit solvent molecules (Figure S7). We performed these calculations in two ways: with methanol added to the already optimised structures of Schiff bases with intramolecular hydrogen bonding where appropriate, and with solvent included in hydrogen bonding between donor–acceptor atoms in investigated compounds. Based on obtained data, one can see that there is no noteworthy influence on the appearance of bands in simulated UV spectra. Namely, as in the case of implicit solvent, all experimental bands are repeated in the simulated spectrum. Also, simulations were done with the extended number of the vertical electronic states, but it did not contribute to any improvement (Figure S7).

Conclusion

In the present study, we examined the UV-Vis absorption spectra of 10 phenolic Schiff bases with both TDDFT and NLMO clusters approaches. The TDDFT/B3LYP method reproduced the experimental values relatively well. According to the NLMO clusters approach, all compounds, except 2, exhibit very similar behaviour. Namely,

the HOMO and HOMO-1 clusters are delocalised over the A or B rings. The HOMO cluster is spread over the electron richer ring (most favourable molecular moiety for electron excitation at long wavelengths), whereas the HOMO-1 cluster is delocalised over the other ring. The influence of the substituents to the electron density of the rings is of crucial importance, as they show different inductive and resonance effects. It was found that in the compounds 3, 4 and 8 the HOMO and HOMO-1 clusters are spread over the B and A ring, respectively. On the other hand, in the Schiff bases 1, 2 and 5–7 the HOMO and HOMO-1 clusters are delocalised over the A and B ring, respectively. A common feature of all examined molecules, except for 2, is that the LUMO cluster is composed of the π^* orbital of the imino group. The two bands at long wavelengths correspond to the HOMO \rightarrow LUMO and HOMO-1 \rightarrow LUMO transitions, i.e. from both rings to the imino group. This finding is in perfect accordance with the results of Amati *et al.* [37] who concluded that both the iminic bridge and aromatic rings are involved in a transition at long wavelengths. These two electronic transitions are characterised with very small energetic and spatial separations. The next band originates from a transition from the imino group to the imino group. Finally, the band at the smallest wavelengths originates from a transition from the A ring to the A ring, or from the B ring to the B ring. The latter two electronic transitions are spatially very favourable, but are characterised with significantly larger energetic separations. Only in the case of the Schiff base 2, the LUMO cluster is positioned on the nitro group, the substituent on the B ring. Since the nitro group decreases electron density in the B ring, the HOMO-1 cluster is spread over this ring, whereas the HOMO cluster is delocalised over the A ring. In spite of the fact that the HOMO \rightarrow LUMO transition is characterised with smaller energetic separation, the HOMO-1 \rightarrow LUMO transition is more favourable, due to significantly smaller spatial separation. Our results confirmed the finding of Marković and Tošović [27] that the TDDFT and NBO theories can be complementarily used to successfully describe electronic transitions in the UV-Vis spectra.

Acknowledgments

This work was supported by the Ministry of Education, Science and Technological Development of the Republic of Serbia (projects No 172016, 174028). The authors are very grateful to the research group of Professor Svetlana Marković for useful advice regarding this work.

Disclosure statement

No potential conflict of interest was reported by the authors.

Funding

Ministry of Education, Science and Technological Development of the Republic of Serbia [project number 172016], [project number 174028].

References

- [1] A. Augustyniak, G. Bartosz, A. Čipak, G. Duburs, L. Horakova, W. Lucuzaj, M. Majekova, A.D. Odysseos, L. Rackova, E. Skrzydlewska, M. Stefek, M. Štrosova, G. Tirzitis, P.R. Venskutonis, J. Viskupicova, P.S. Vranka, and N. Žarković, *Free Radical Res.* **44**, 1216 (2010).
- [2] B. Halliwell and J.M.C. Gutteridge, *Free Radicals in Biology and Medicine*, 3rd ed. (Clarendon Press, Oxford, 1999).
- [3] I. Fridovich, *Science* **20**, 875 (1978).
- [4] H. Sies, editor. *Oxidative Stress. Oxidants and Antioxidants* (Academic Press, New York, 1991).
- [5] C.E. Thomas and B. Kalyanaraman, *Oxygen Radicals and the Disease Process* (Harwood Academic Publishers, Reading, UK, 1998).
- [6] B. Halliwell, *Free Radicals and Other Reactive Species in Disease; Encyclopedia of Life Sciences* (Nature Publishing Group, London, UK, 2001).
- [7] J.W. Powles and A.R. Ness, *Int. J. Epidemiol.* **26**, 1 (1997).
- [8] R.A. Jacob and B. Burri, *J. Am. Jaclyn. Nutr.* **63**, 985S (1996).
- [9] G. Block, B. Patterson, and A. Subar, *Nutr. Cancer* **18**, 1 (1992).
- [10] M.T. Huang, C.T. Ho, and C.Y. Lee, editors. *Phenolic Compounds in Food and Their Effects on Health II, Antioxidants and Cancer Prevention* (American Chemical Society, Washington, DC, 1992), p. 8.
- [11] C. Rice-Evans, N.J. Miller, and G. Paganga, *Free Radic Biol Med.* **20**, 933 (1996).
- [12] B. Halliwell, R. Aeschbach, J. Loliger, and O.I. Aruoma, *Food Chem. Toxicol.* **33**, 601 (1995).
- [13] E. Anouar, C. Calliste, P. Kosinova, F. Di Meo, J. Duroux, Y. Champavier, K. Marakchi, and P. Trouillas, *J. Phys. Chem. A* **113**, 13881 (2009).
- [14] H. Schiff, *Justus Liebigs Ann. Chem.* **131**, 118 (1864).
- [15] W. Radecka-Paryzek, I. Pospieszna-Markiewicz, and M. Kubicki, *Inorg. Chim. Acta* **360**, 488 (2007).
- [16] R.H. Lozier, R.A. Bogomolni, and W. Stoeckenius, *Biophys. J.* **15**, 955 (1975).
- [17] E.M. Hodnett and W.J. Dunn, *J. Med. Chem.* **13**, 768 (1970).
- [18] C.M. Silva da, D.L. Silva da, L.V. Modolo, R.B. Alves, M.A. de Resende, C.V.B. Martins, and Á. de Fátima, *J. Adv. Res.* **2**, 1 (2011).
- [19] X.-B. Yang, Q. Wang, Y. Huang, P.-H. Fu, J.-S. Zhang, and R.-Q. Zeng, *Inorg. Chem. Commun.* **25**, 55 (2012).
- [20] K. Brodowska and E. Lodyga-Chruscinska, *Chemik* **68**, 129 (2014).
- [21] L.X. Chenga, J.-J. Tanga, H. Luob, X.-L. Jina, F. Dai, J. Yanga, Y.-P. Qiana, X.-Z. Li, and B. Zhoua, *Bioorg. Med. Chem. Lett.* **20**, 2417 (2010).
- [22] K.K. Upadhyay, A. Kumar, S. Upadhyay, and P.C. Mishra, *J. Mol. Struct.* **873**, 5 (2008).
- [23] Z.D. Petrović, J. Đorović, D. Simijonović, V. Petrović, and Z. Marković, *RSC Adv.* **5**, 24094 (2015).

- [24] Z. Marković, J. Đorović, Z.D. Petrović, V. Petrović, and D. Simijonović, *J. Mol. Model.* **21**, 293 (2015).
- [25] J.B. Harborne, T.J. Mabry, and H. Mabry, *The Flavonoids*. (Chapman and Hall, London, 1975).
- [26] M.E. Casida, *J. Mol. Struct.: THEOCHEM* **914**, 3 (2009).
- [27] S. Marković and J. Tošović, *J. Phys. Chem. A* **119**, 9352 (2015).
- [28] M.J. Frisch, G.W. Trucks, H.B. Schlegel, G.E. Scuseria, M.A. Robb, J.R. Cheeseman, G. Scalmani, V. Barone, B. Mennucci, G.A. Petersson, H. Nakatsuji, M. Caricato, X. Li, H.P. Hratchian, A.F. Izmaylov, J. Bloino, G. Zheng, J.L. Sonnenberg, M. Hada, M. Ehara, K. Toyota, R. Fukuda, J. Hasegawa, M. Ishida, T. Nakajima, Y. Honda, O. Kitao, H. Nakai, T. Vreven, J.A. Montgomery, Jr., J.E. Peralta, F. Ogliaro, M. Bearpark, J.J. Heyd, E. Brothers, K.N. Kudin, V.N. Staroverov, T. Keith, R. Kobayashi, J. Normand, K. Raghavachari, A. Rendell, J.C. Burant, S.S. Iyengar, J. Tomasi, M. Cossi, N. Rega, J.M. Millam, M. Klene, J.E. Knox, J.B. Cross, V. Bakken, C. Adamo, J. Jaramillo, R. Gomperts, R.E. Stratmann, O. Yazyev, A.J. Austin, R. Cammi, C. Pomelli, J.W. Ochterski, R.L. Martin, K. Morokuma, V.G. Zakrzewski, G.A. Voth, P. Salvador, J.J. Dannenberg, S. Dapprich, A.D. Daniels, O. Farkas, J.B. Foresman, J.V. Ortiz, J. Cioslowski, and D.J. Fox, Gaussian 09, Revision C.01 (Gaussian, Inc., Wallingford, CT, 2010).
- [29] C. Lee, W. Yang, and R.G. Parr, *Phys. Rev. B: Condens. Matter Mater. Phys.* **37**, 785 (1988).
- [30] A.D. Becke, *J. Chem. Phys.* **98**, 5648 (1993).
- [31] M. Ernzerhof and G.E. Scuseria, *J. Chem. Phys.* **110**, 5029 (1999).
- [32] Y. Zhao, N.E. Schultz, and D.G. Truhlar, *J. Chem. Phys.* **123**, 161103 (2005).
- [33] M. Cossi, N. Rega, G. Scalmani, and V. Barone, *J. Comput. Chem.* **24**, 669 (2003).
- [34] V.M. Jiménez-Pérez, B.M. Muñoz-Flores, L.M. Blanco Jerez, A. Gómez, L.D. Rangel, R. Chan-Navarro, N. Waksman, and R. Ramírez-Durón, *Int. J. Electrochem. Sci.* **9**, 7431 (2014).
- [35] A. Cinarli, D. Gürbüz, A. Tavman, and A. Seher Birteksöz, *Bull. Chem. Soc. Ethiopia* **25**, 407 (2011).
- [36] P.S. Kalsi, *Spectroscopy of Organic Compounds*, 6th ed. (New Age International Ltd, New Delhi, 2007).
- [37] A. Amati, C. Bonini, M. D'Auria, M. Funicell, F. Lelj, and R. Racioppi, *J. Org. Chem.* **71**, 7165 (2006).
- [38] J. Autschbach, *ChemPhysChem* **10**, 1757 (2009).